Regenerative Therapy 19 (2022) 77–87

Contents lists available at ScienceDirect

Regenerative Therapy

journal homepage: http://www.elsevier.com/locate/reth

Original Article

Transplantation of a human induced pluripotent stem cell-derived airway epithelial cell sheet into the middle ear of rats

Takeshi Tada [a, b], Hiroe Ohnishi [a], Norio Yamamoto [a, *], Fumihiko Kuwata [a], Yasuyuki Hayashi [a], Hideaki Okuyama [a, c], Tsunetaro Morino [b], Yoshiyuki Kasai [b], Hiromi Kojima [b], Koichi Omori [a]

[a] Department of Otolaryngology-Head and Neck Surgery, Graduate School of Medicine, Kyoto University, 54 Shogoin Kawahara-cho, Sakyo-ku, Kyoto City, Kyoto 606-8507, Japan
[b] Department of Otorhinolaryngology, Jikei University School of Medicine, 3-25-8 Nishi-Shimbashi, Minato-ku, Tokyo 105-8461, Japan
[c] School of Communication Sciences and Disorders, McGill University, Montreal, QC H3A 1G1, Canada

ARTICLE INFO

Article history:
Received 4 November 2021
Received in revised form
26 December 2021
Accepted 2 January 2022

Keywords:
Cholesteatoma
Induced pluripotent stem cell
Middle ear
Otitis media
Transplantation

ABSTRACT

Introduction: Early postoperative regeneration of the middle ear mucosa is essential for the prevention of postoperative refractory otitis media and recurrent cholesteatoma. As a means for intractable otitis media management, we focused on human induced pluripotent stem cell (hiPSC)-derived airway epithelial cells (AECs), which have been used in upper airway mucosal regeneration and transplantation therapy. In this study, we transplanted hiPSC-derived AECs into the middle ear of immunodeficient rats.
Methods: Following the preparation of AEC sheets from hiPSCs, the bilateral middle ear mucosa of X-linked severe combined immunodeficient rats was scraped, and the AEC sheets were transplanted in the ears unilaterally.
Results: Human nuclear antigen (HNA)-positive ciliated cells were observed on the transplanted side of the middle ear cavity surface in three of six rats in the 1-week postoperative group and in three of eight rats in the 2-week postoperative group. No HNA-positive cells were found on the control side. The percentage of HNA-positive ciliated cells in the transplanted areas increased in the 2-week postoperative group compared with the 1-week group, suggesting survival of hiPSC-derived AECs. Additionally, HNA-positive ciliated cells were mainly located at sites where the original ciliated cells were localized. Immunohistochemical analysis showed that the transplanted AECs contained cytokeratin 5- and mucin 5AC-positive cells, indicating that both basal cells and goblet cells had regenerated within the middle ear cavity.
Conclusions: The results of this study are an important first step in the establishment of a novel transplantation therapy for chronic otitis media.

1. Introduction

The middle ear is a functional organ that requires sufficient aeration to efficiently transmit sound from the external auditory canal to the cochlea and auditory nerve. It is composed of a tympanic cavity, an epitympanum, and a mastoid cavity. The Eustachian tube (ET) connects the tympanic cavity and nasopharynx. Aeration within the middle ear is maintained via two mechanisms: direct aeration through the ET and gas exchange to the blood vessels through the middle ear epithelia [1]. Inflammation within the middle ear (chronic otitis media) causes ET obstruction and loss of gas exchange due to epithelial dysfunction, which results in negative pressure within the middle ear. This negative pressure can be resolved with chronic perforation of the tympanic membrane and/

Abbreviations: Ac-TUB, acetylated α-tubulin; AEC, airway epithelial cell; CPM, carboxypeptidase M; DAPI, 4′,6-diamidino-2-phenylindole; EDTA, ethylenediaminetetraacetic acid; ET, Eustachian tube; hiPSC, human induced pluripotent stem cell; HNA, human nuclear antigen; KRT5, cytokeratin5; MUC5AC, mucin5AC; NBRP, National BioResource Project; OCT, optimal cutting temperature; PBS, phosphate-buffered saline; PET, polyethylene terephthalate; PFA, paraformaldehyde; X-SCID, x-linked severe combined immunodeficient.

* Corresponding author. Department of Otolaryngology-Head and Neck Surgery, Graduate School of Medicine, Kyoto University, 54 Shogoin Kawahara-cho, Sakyo-ku, Kyoto City, Kyoto, 606-8507, Japan. Fax: +81 75 751 7225.
E-mail addresses: t.tada@jikei.ac.jp (T. Tada), h_oonishi@ent.kuhp.kyoto-u.ac.jp (H. Ohnishi), yamamoto@ent.kuhp.kyoto-u.ac.jp (N. Yamamoto), f_kuwata@ent.kuhp.kyoto-u.ac.jp (F. Kuwata), yasuyuki_hayashi@ent.kuhp.kyoto-u.ac.jp (Y. Hayashi), hideaki.okuyama@mail.mcgill.ca (H. Okuyama), moritune@jikei.ac.jp (T. Morino), ykasai@jikei.ac.jp (Y. Kasai), kojimah@jikei.ac.jp (H. Kojima), omori@ent.kuhp.kyoto-u.ac.jp (K. Omori).

Peer review under responsibility of the Japanese Society for Regenerative Medicine.

https://doi.org/10.1016/j.reth.2022.01.001

or causes retraction of the tympanic membrane, known as cholesteatoma. If cholesteatoma grows with continuous negative pressure, it can destroy the bony structure within the middle ear, including the ossicles, facial nerve canals, and inner ear [2]. The mucosa of the middle ear cavity is one of the mucociliary epithelia and it has phenotypic similarities to the conducting airway epithelium, which consists of pseudostratified columnar epithelia that includes ciliated, secretory, non-secretory, and basal cells [3]. The ciliated and secretory cells are mainly located in the inferior tympanic cavity and around the opening of the ET. These cells produce mucus that flows toward the ET and helps to discharge foreign substances within the middle ear secretions toward the nasopharynx. On the other hand, the mucosa of the mastoid and superior tympanic cavities is mainly responsible for passive gas exchange [1] to ensure middle ear aeration; therefore, few ciliated and secretory cells are located in these areas. The surgical management of both chronic otitis media and cholesteatoma not only removes pathological lesions but also a normal middle ear mucosa in both the tympanic and mastoid cavities, which can result in worse postoperative mucosal conditions compared with the preoperative status. Generally, it is believed that mucosal tissues can regenerate easily; however, this is not always the case in widespread middle ear mucosal defects associated with the treatment of chronic otitis media and cholesteatoma. The incomplete regeneration and remodeling of the middle ear mucosa cause poor aeration of the middle ear cavity, resulting in tympanic membrane adhesion, fibrosis, and cholesteatoma, or otitis media recurrence [4]. Additionally, insufficient hearing recovery occurs because of poor aeration of the postoperative middle ear [5]. A silastic sheet and cartilage tissue are used to prevent adhesion [6,7]; however, these methods only partially contribute to the functional recovery of the middle ear. Thus, an effective method for restoring the functional middle ear mucosa that realizes reliable aeration within the postoperative middle ear and fundamentally resolves tympanic membrane adhesions is required.

Middle ear mucosal regeneration involves the removal of the pathological mucosa by surgical means followed by transplantation of the physiological mucosa to restore mucosal function in the early postoperative period [8]. Previous reports have shown effectiveness of transplanting autologous tissue-derived “nasal mucosal cell sheets”, which are a different type of airway epithelium, into the middle ear to achieve early postoperative mucosal regeneration [9–11]. However, two issues associated with nasal mucosa use remain unaddressed. The first is its invasiveness; to obtain the nasal mucosal cell sheet, the patient's healthy nasal mucosa needs to be excised. And second, the cultured nasal cavity epithelia have different characteristics from the middle ear epithelia. Although the cultured nasal cavity epithelia show a multilayered structure and allow gas exchange, they do not contain ciliated cells that are present in the middle ear mucosa [9–11]. This difference results in inadequate functioning of the transplanted nasal epithelia in the middle ear, especially in the tympanic cavity and around the ET, where ciliated cells have important roles. Therefore, in this study, we used human induced pluripotent stem cell (hiPSC)-derived airway epithelial cells (AECs); compared to autologous nasal tissue, these cells are rich in cilia which additionally contribute to motility.

hiPSCs are expected to be clinically applicable using human leukocyte antigen-type-matched cell banks [12–14], allowing patients to benefit from transplantation without eliciting an immune response, even if the hiPSCs are derived from other patients. There have been no reports regarding the creation of middle ear mucosa from pluripotent stem cells; however, recent single-cell transcriptome studies [15–17] and conventional electron microscopic reports [3,18] support the existence of five types of mucociliary cells in the middle ear mucosa [15], similar to other respiratory tract mucosae like trachea and nasal cavity [17]. Thus, we decided to use a previously reported protocol to induce lower AECs, which are rich in motor cilia, from hiPSCs [19,20]. These cells were used as the cellular source for transplantation into the middle ear cavity, as has already been performed for the regeneration of rat tracheal epithelia [21].

In this study, we developed and explored a novel middle ear mucosal regeneration method; specifically, we transplanted hiPSC-derived AECs into the middle ear of immunodeficient rats.

2. Methods

2.1. Animals

X-linked severe combined immunodeficient (X-SCID) rats (F344-*Il2rg*^{em1lexas}, NBRP No. 0883) were provided by the National BioResource Project (NBRP) — Rat, University of Tokyo (Tokyo, Japan). The rats were 7–17 weeks old and weighed 174–330 g. Sixteen rats with an equal sex distribution were used. This study was approved by the Animal Research Committee, Graduate School of Medicine, Kyoto University (MedKyo17627). All animal experiments were performed in accordance with the National Institutes of Health guide for the care and use of Laboratory animals.

2.2. Maintenance of hiPSCs and AEC induction

The hiPSC line 201B7 was used in this study and was provided by RIKEN BRC through the NBRP of the MEXT/AMED, Japan. hiPSC maintenance and induction of airway cells were performed, as described previously [19,20]. Briefly, before induction, the cells were maintained on Geltrex (Thermo Fisher Scientific, Waltham, MA, USA)-coated dishes in Essential 8 medium (Thermo Fisher Scientific) for ten passages. Passaging was performed using 0.5 mM ethylenediaminetetraacetic acid (EDTA)/phosphate-buffered saline (PBS) with a split ratio of 1:10.

To initiate AEC induction, the hiPSCs were seeded on Geltrex-coated plates in basal medium 1 (RPMI1640 medium [Nacalai Tesque, Kyoto, Japan] with 1 × B27 supplement [Thermo Fisher Scientific] and 50 U/mL penicillin [Thermo Fisher Scientific]/50 μg/mL streptomycin [Thermo Fisher Scientific]) containing 100 ng/mL human activin A (R&D System, Minneapolis, MN, USA), 1 μM CHIR99021 (Axon Medchem, Groningen, The Netherlands), and 10 μM Y-27632 (FUJIFILM Wako Pure Chemical Corporation, Osaka, Japan). On the next day, 0.25 mM sodium butyrate (FUJIFILM Wako Pure Chemical Corporation) was added. From day 2–6, cells were cultured in basal medium 1 containing 100 ng/mL human activin A, 1 μM CHIR99021, and 0.125 mM sodium butyrate. From day 6–10, cells were cultured in basal medium 2 (DMEM/F-12 with GlutaMAX [Thermo Fisher Scientific], 1 × B27 supplement, 50 U/mL penicillin/50 μg/mL streptomycin, 0.05 mg/mL L-ascorbic acid [FUJIFILM Wako Pure Chemical Corporation], and 0.4 mM monothioglycerol [FUJIFILM Wako Pure Chemical Corporation]) supplemented with 100 ng/mL human recombinant noggin (Human Zyme, Chicago, IL, USA) and 10 μM SB431542 (Selleck Chemicals, Houston, TX, USA). From day 10–14, the cells were cultured in basal medium 2 containing 20 ng/mL human recombinant BMP4 (Human Zyme), 2.5 μM CHIR99201, and 0.5 μM all-trans retinoic acid (Sigma—Aldrich, St. Louis, MO, USA).

Carboxypeptidase M (CPM) is a marker for primitive cells in the ventral anterior foregut that develops into the bronchi and lungs [19,21]. On day 14, CPM-positive cells were selected by a magnetically activated cell sorting method using a mouse anti-human CPM antibody (FUJIFILM Wako Pure Chemical Corporation). CPM-positive cells were mixed in a solution of 1:1 growth factor-reduced Matrigel (Corning, Corning, NY, USA) and basal medium

2 containing 3.0 μM CHIR99021, 100 ng/mL FGF10 (FUJIFILM Wako Pure Chemical Corporation), and 10 μM Y-27632 and were seeded on 12-well cell culture inserts with a polyethylene terephthalate (PET) membrane (Corning, #353292). For 14 days, Matrigel embedded cells were maintained in basal medium 2 containing 3.0 μM CHIR99021, 100 ng/mL FGF10, and 10 μM Y-27632. From day 28–42, spheroids-derived from CPM-positive cells were cultured in PneumaCult-ALI Maintenance medium (STEMCELL Technologies, Vancouver, Canada) with 10 μM Y-27632, 4 μg/mL heparin (Nacalai Tesque), 1 μM hydrocortisone (Sigma–Aldrich), and 10 μM DAPT (FUJIFILM Wako Pure Chemical Corporation). On day 42, the spheroids were dissociated into a single-cell suspension by treatment with trypsin, seeded on 12-well cell culture inserts with a PET membrane, and maintained under air-liquid interface culture condition. After 14 days of culturing, the induced AEC sheets were used for transplantation (Fig. 1).

2.3. Electron microscopy

Induced AECs on the PET membrane before transplantation and F344 wild-type rat middle ear mucosa were observed using scanning and transmission electron microscopes. For scanning electron microscopy (S-4700 [Hitachi Co., Tokyo, Japan]), the cells were fixed with 4% paraformaldehyde (PFA) (Nacalai Tesque)/2% glutaraldehyde (FUJIFILM Wako Pure Chemical Corporation) in phosphate buffer at 4 °C overnight. Then, the cells were post-fixed in 1% osmium tetroxide (Nacalai Tesque), dehydrated, dried using a critical point drying method, and coated with platinum palladium. For transmission electron microscopy (H-7650, Hitachi Co.), the fixed cells were post-fixed in 1% osmium tetroxide for 2 h and dehydrated using an ethanol series. The cells were then embedded in epoxy resin and DMP-30 (Nacalai Tesque). Thin sections were stained with uranyl acetate (Merck Millipore, Burlington, MA, USA) and lead citrate (Nacalai Tesque).

2.4. Transplantation

The rats were anesthetized intraperitoneally using a mixture of midazolam (2 mg/kg, Maruishi Pharmaceutical Corporation, Osaka, Japan), butorphanol (2.5 mg/kg, Meiji Seika Pharma Corporation, Tokyo, Japan), and medetomidine (0.15 mg/kg, Orion Corporation, Espoo, Finland). Transplant operations were performed under a stereoscopic microscope (LW-820; WRAYMER, Osaka, Japan) in a sterile tent (PS01-AD; AS ONE Corporation, Tokyo, Japan). Fourteen X-SCID rats were used as transplant recipients; the additional two were used as controls. The induced cells were detached from their scaffold, the PET membrane, and transplanted into the middle ear mucosal defects. The surgical approach to the middle ear cavity was based on previous reports [22–24]. An incision was performed on the retro-auricular skin measuring approximately 3 cm; the flaps were raised under a platysma layer to identify and preserve the facial nerve. The auditory bulla was exposed, and a surgical window was created on its lateral posterior surface. The size of the surgical window was 3 mm and 1.5 mm in length and width, respectively, and was located between the facial nerve and mastoid process. The area of peeling of the middle ear mucosa was defined as

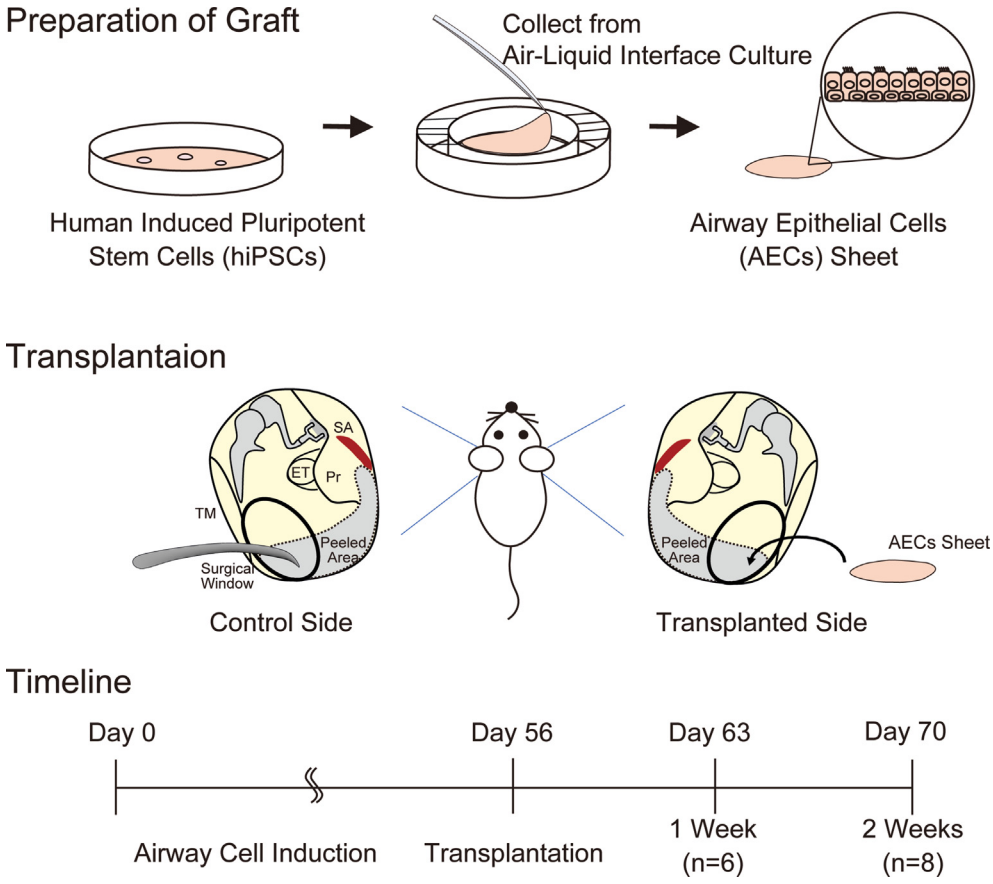

Fig. 1. Scheme of the experimental design. **Preparation of the graft**. Airway epithelial cells (AECs) were induced from human induced pluripotent stem cells (hiPSCs) and were collected from a culture insert with a PET membrane as a sheet. **Transplantation**. The bilateral middle ear mucosae of X-linked severe combined immunodeficient rats were peeled under general anesthesia. The induced AEC sheet was transplanted to one side of the middle ear. **Timeline**. Postoperative wound status was compared between the control and transplanted sides after 1 (n = 6) and 2 weeks (n = 8). ET, eustachian tube; Pr, promontory; SA, stapedial artery; TM, tympanic membrane.

surrounding stapedial artery at the posterior end, the lateral edge of the promontory at the medial end, and we defined the area visible from the surgical window as the lateral and anterior ends (Fig. 1). The bilateral middle ear mucosae of the hypotympanum were detached, and the coordinated hiPSC-derived airway cell sheet was transplanted unilaterally. Finally, the skin wound was sutured using 5.0 nylon sutures. Two rats were not operated on and served as the control group. Histological evaluation was performed after one (experimental animals: n = 6) and two weeks (experimental animals: n = 8) after surgery in the intervention group (Fig. 1), and for control animals (n = 2).

2.5. Immunofluorescent staining

One to two weeks post-transplantation, the rats were euthanized in accordance with the regulations of Kyoto University. The temporal bone, including the auditory bullae, were fixed in 4% PFA at 4 °C for 24 h and decalcified with 10% EDTA-Na for 7 days. The samples were immersed in 30% sucrose overnight, followed by overnight immersion in a 1:1 mixed solution of 30% sucrose and Tissue-Tec optimal cutting temperature (OCT) compound (Sakura Finetek Japan, Tokyo, Japan). The samples were then embedded in the OCT compound. The auditory bullae were sliced in the coronal direction at a 10 μm thickness using a cryostat (CryoStar NX70, Thermo Fisher Scientific). Cultured cells were fixed in 4% PFA for 15 min at room temperature. After washing with PBS, all specimens were permeabilized with 0.2% Triton X-100 (Nacalai Tesque) in PBS for 5 min. The samples were incubated with 1% bovine serum albumin (FUJIFILM Wako Pure Chemical Corporation) in PBS for 10 min at room temperature and were stained with primary antibodies at 4 °C overnight. After washing with PBS, the sections were incubated with Alexa Fluor secondary antibodies (Thermo Fisher Scientific) and phalloidin 647 (1:1000, Thermo Fisher Scientific) for 1 h at room temperature. Nuclei were labeled with 4′,6-diamidino-2-phenylindole (DAPI; Thermo Fisher Scientific). The primary antibodies used in this study were anti-FOXA2 antibody (1:500, R&D Systems, AF2400), anti-NKX2-1 antibody (1:500, Thermo Fisher Scientific, MS-699-P), anti-E-cadherin antibody (1:10000, Thermo Fisher Scientific, 13-1900), anti-acetylated α-tubulin (Ac-TUB) antibody (1:1000, Sigma–Aldrich, T7451), anti-human nuclei antigen (HNA) antibody (1:1000, Millipore, Darmstadt, Germany, MAB1281), anti-mucin5AC (MUC5AC) antibody (1:500, Thermo Fisher Scientific, MS-145-P), and anti-cytokeratin5 (KRT5) antibody (1:1000, BioLegend, San Diego, CA, USA Poly19055). For double-staining with anti-MUC5AC and anti-HNA antibodies, a direct labeling kit (1:500, Thermo Fisher Scientific, Z25060) was used according to the manufacturer's protocol. The specimens were enclosed in Fluoromount-G® Anti-Fade (Southern Biotechnology Associates Inc., Birmingham, AL, USA). Other tissue specimens were stained with hematoxylin (FUJIFILM Wako Pure Chemical Corporation) and eosin (FUJIFILM Wako Pure Chemical Corporation) and enclosed by a sealing agent (Mount-Quick, Cosmobio, Tokyo, Japan).

Specimens were observed and images were visualized using a BioRevo fluorescent microscope BZ-9000 (Keyence, Osaka, Japan) and an Olympus BX50 microscope (Olympus, Tokyo, Japan); images were captured with an Olympus DP70 digital camera (Olympus). The images of cultured cells were visualized using a Nikon Eclipse Ti inverted microscope (Nikon, Tokyo, Japan) and captured with an Olympus DP73 digital camera (Olympus). Digital images were processed using Photoshop 2021 (Adobe, San Jose, CA, USA).

2.6. Cell count

All quantification procedures were performed on immunofluorescent sections. Epithelial cells were defined as the cells located in the most luminal monolayer marked by phalloidin. The surviving transplanted cell-derived epithelial cells were labeled and identified using anti-HNA antibody and DAPI. First, the number of surviving cells was counted in whole areas where the middle ear mucosae were peeled. The proportion of surviving cells was calculated by dividing the number of HNA- and DAPI-double-positive cells by the number of DAPI-positive cells. On the same slide, the number of Ac-TUB and HNA double-positive cells was quantified among the HNA-positive epithelial cells. Additionally, the transplanted HNA-positive cells and Ac-TUB- and HNA-double-positive cells were quantified within 350 μm of regions of the expected ciliated and non-ciliated part of the peeled mucosal area in each specimen. Specimens from both ears of rats (n = 16) were quantified in ten sections at 200 μm intervals. We averaged the proportions of the different ears to identify the statistical difference.

2.7. Statistical analysis

Data are expressed as median (range; minimum–maximum value). The Wilcoxon signed-rank test was used to compare the proportion of ciliated cells in the ciliated and non-ciliated part. The Wilcoxon rank sum test was used to examine the difference of the proportion of transplanted cells among epithelial cells and ciliated cells among the transplanted cells. Statistical significance was set at $p < 0.05$. Statistical analysis was performed using R version 3.0.2 (2013-09-25).

3. Results

3.1. AEC induction

AEC induction was performed as previously reported [19,20]. At each induction step, marker protein expression was confirmed by immunocytochemical analyses (Supplementary Fig. 1). On days 56–60, the induction of AECs was confirmed by the expression of an epithelial marker (E-cadherin) and a cilia marker (Ac-TUB) (Fig. 2a). Cilia-like structures were observed using scanning electron microscopy (Fig. 2b). In transmission electron microscopy, 9 + 2 structures were observed in cilia-like protrusions, as reported previously (Fig. 2c) [20]; these structures were composed of nine doublet microtubules arranged in a circle around two central singlet microtubules with dynein arms [25].

3.2. Ciliated cells were abundantly located near the cochlea and stapedial artery in the rat middle ear cavity

To select appropriate implantation sites for AECs, we examined the ciliated cell distribution in the middle ear mucosa of X-SCID rats and F344 rats, the background strain animals of X-SCID, based on assumption that the ciliated cell-rich part would require the compensation with transplanted AECs after injury compared with non-ciliated area and would be a target for regeneration of the middle ear mucosa (Fig. 3). Similar to a report of Sprague–Dawley rats [26], scanning electron microscopy revealed that ciliated cells in F344 rats were abundant around the cochlea and the stapedial artery (Fig. 3a–c). In the histological sections of the middle ear cavity of X-SCID rats (Fig. 3d–g), the distribution of Ac-TUB-positive ciliated cells was shown to be limited to the area around the stapedial artery and cochlea (ciliated part, green region in Fig. 3d, solid box in Fig. 3e, and 3f); a sparse distribution was observed in the region apart from the artery or cochlea (non-ciliated part, yellow region in Fig. 3d, dotted box in Fig. 3e, and 3g). Similar to the report in Sprague–Dawley rats, we confirmed that X-SCID rats have both ciliated (Fig. 3f) and non-ciliated areas (Fig. 3g). Based on these

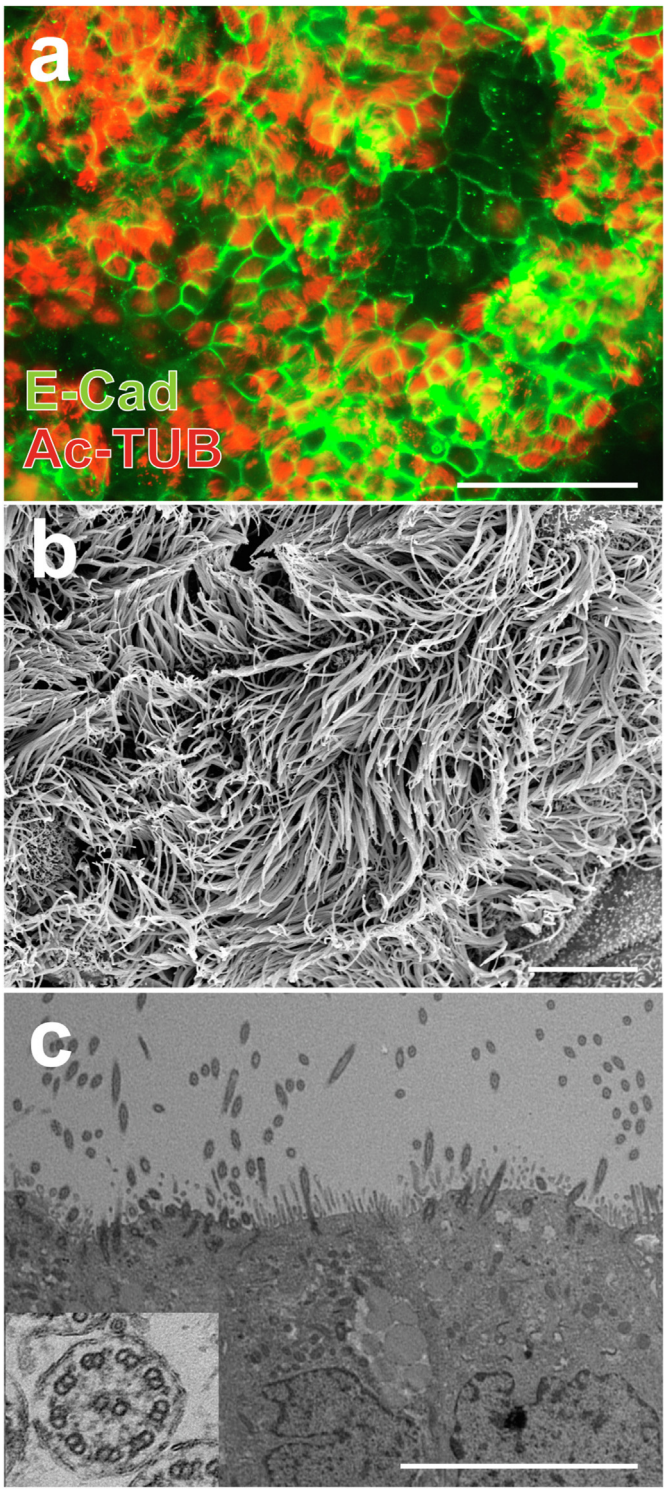

Fig. 2. hiPSC-derived AEC contain ciliated cells before transplantation. (a) Immunofluorescence analyses showed the expression of E-cadherin (E-Cad) and acetylated α-tubulin (Ac-TUB) in hiPSC-derived AECs. Scale bar = 100 μm. (b) Scanning electron microscopy images showed cilia-like structures in hiPSC-derived AECs. Scale bar = 80 μm. (c) Transmission electron microscopy images showed a "9 + 2" structure (inset), which was observed specifically in motile cilia, in cilia-like protrusions within hiPSC-derived AECs. Scale bar = 10 μm hiPSC, human induced pluripotent stem cells; AECs, airway epithelial cells.

observations, a surgical window was created to observe the region of the middle ear cavity surrounded by the cochlea and stapedial artery (light green area in Fig. 3a). The protocol for the transplantation procedure was as follows: first, we created a surgical window over the region surrounded by the cochlea and stapedial artery (black circle in Fig. 3a); next, we peeled the mucosa from the stapedial artery and cochlea to the edge of the surgical window (dotted line in Fig. 3a) and transplanted an hiPSC-derived AEC sheet over the peeled area.

3.3. Transplanted cell survival in the middle ear

The histological structure of the transplanted side was different compared with that of the control side, in which only the mucosa was removed (Supplementary Fig. 2). The injured region of the control side showed bony thickening of the tissue (Supplementary Fig. 2a, c), which was similar to that in normal rabbits in previous studies [9,10]. In contrast, the transplanted side contained sparse connective tissue under the epithelial cells (Supplemental Fig. 2b, d), which was not observed in the transplantation of autologous tissues [9,10].

Immunofluorescent staining was performed to examine the status of the transplanted hiPSC-derived AEC sheets in the middle ear cavity (Fig. 4). HNA and Ac-TUB were immunohistochemically stained to identify hiPSC-derived cells and ciliated cells, respectively. HNA-positive cells were confirmed on the surface of the middle ear cavity in five of six animals in the 1-week postoperative group and three of eight animals in the 2-week postoperative group (Fig. 4a, c–g). HNA and Ac-TUB double-positive cells were observed in the middle ear cavity surface in three of six animals in the 1-week postoperative group and three of eight animals in the 2-week postoperative group. Additionally, no HNA-positive cells were observed in control ears (Fig. 4b, h). Although HNA-positive cells were also observed in the submucosa (Fig. 4a), we focused on the analysis of epithelial cells, which are the functional cells within the middle ear.

The number of transplanted epithelial layer cells was quantified in the whole peeled area to evaluate the survival of engrafted cells at the transplant site (Fig. 5). The median percentage of HNA-positive cells among the epithelial cells in the whole mucosal defect area was 8.87% (0.00–43.69%) in the 1-week group (n = 6) and 0.00% (0.00–6.14%) in the 2-week group (n = 8) (Fig. 5g, whole peeled area). The proportion of HNA-positive epithelial cells in the 2-week group was significantly reduced compared with that in the 1-week group (p = 0.0266, Fig. 5g, whole peeled area). Furthermore, the proportion of ciliated cells among transplanted cells engrafted on the surface of the middle ear cavity was 1.00% (0.00–3.93% in the 1-week group [n = 5] and 2.99% [2.68–5.88%] in the 2-week group [n = 3]) (Fig. 5h, whole peeled area). However, no significant difference was observed regarding the proportion of ciliated cells between the two groups.

To evaluate the effect of the transplanted site on the survival of transplanted cells, the survival of transplanted epithelial cells and ciliated cells within the expected ciliated and non-ciliated parts was evaluated (Fig. 5g and h, ciliated and non-ciliated parts). The median percentage of surviving transplanted cells in the epithelial layer in the expected ciliated part was 3.74% (0.00–56.84%) in the 1-week group (Fig. 5b and g, ciliated part, n = 6) and 0.00% (0.00–21.76%) in the 2-week group (Fig. 5e and g, ciliated part, n = 8). The median proportion of HNA-positive cells in the expected non-ciliated part was 11.18% (0.00–49.15%) in the 1-week group (Fig. 5c and g, non-ciliated part, n = 6) and 0.00% (0.00–1.39%) in the 2-week group (Fig. 5f and g, non-ciliated part, n = 8). A significant decrease was observed in the survival of transplanted cells in the non-ciliated part in the 2-week group compared to that in the 1 week-group (p = 0.0053), indicating that the decrease in the total number of surviving transplanted cells was mainly due to the cells in the non-ciliated part. In the expected ciliated part, the

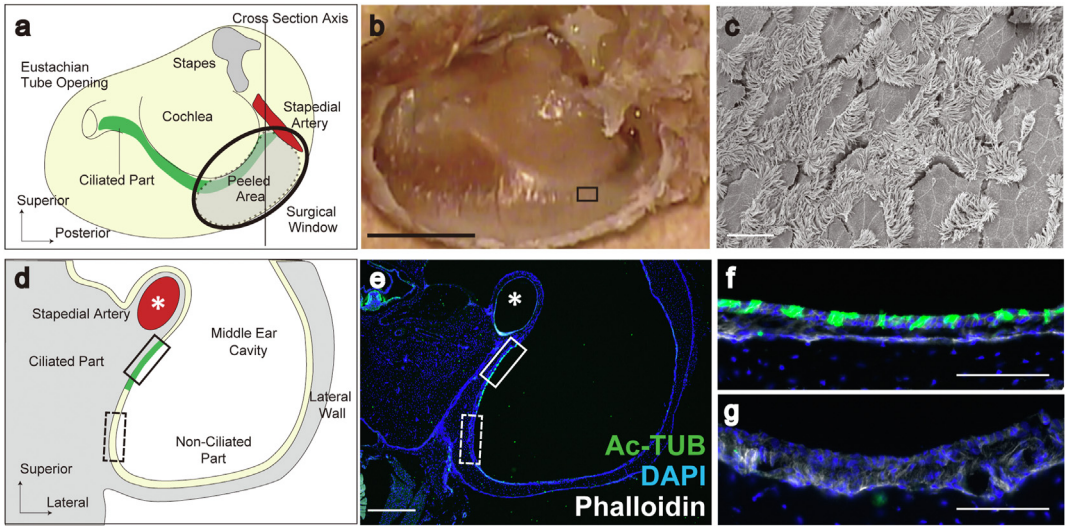

Fig. 3. Middle ear ciliated part. (a) A schema of the middle ear after removing the lateral wall of the middle ear cavity. The gray area surrounded by a dotted line shows an area where the mucosa was peeled in the transplantation experiments. This procedure was performed through the surgical window (black circle) created on the lateral wall of the middle ear cavity. The green and yellow colors indicate the regions of ciliated and non-ciliated cells, respectively. The axis of the histological section in d–g is indicated by the solid line. (b) Macroscopic image of a. Scale bar = 2 mm. (c) Scanning electron microscopy image of the boxed region in b showing the distribution of ciliated structures around the cochlea. Scale bar = 100 μm. (d and e) A schema (d) and an immunohistological section (e) of the middle ear through the solid line indicated in a. Acetylated α-tubulin (Ac-TUB) positive cells, colored in green, located near the stapedial artery (*) as indicated by the solid box. The area far from the artery (dotted box) showed small numbers of Ac-TUB positive cells. Scale bar in e = 500 μm. (f) Magnified image of the solid box (ciliated part) in e. Scale bar = 100 μm. (g) Magnified image of the dotted box (non-ciliated part) in e. Scale bar = 100 μm.

median proportion of Ac-TUB and HNA double-positive cells in the HNA-positive cells was 0.00% (0.00–4.52%) in the 1-week group (Fig. 5b and h, ciliated part, n = 5) and 3.80% (3.05–7.55%) in the 2-week group (Fig. 5e and h, ciliated part, n = 3). In the ciliated part, no significant difference was observed between the two groups; however, the proportion of hiPSC-derived ciliated cells tended to increase in the expected ciliated part in the 2-week group compared to that in the 1-week group. On the other hand, the proportion of Ac-TUB and HNA double-positive cells in the HNA-positive cells engrafted at the expected non-ciliated part was 0.00% (0.00–2.82%) in the 1-week group (Fig. 5c and h, n = 5) and 0.00% (0.00–0.00%) in the 2-week group (Fig. 5f and h, n = 1). HNA-positive cells showed minimal survival in the expected non-ciliated part of the 2-week group after transplantation.

3.4. Transplanted cells contained KRT5-and MUC5AC-positive cells

The airway epithelium is mainly composed of ciliated cells, goblet cells, and basal cells [27,28]. Immunohistochemistry for KRT5, a middle ear mucosa basal cell marker [29,30], and MUC5AC, a goblet cell marker expressed in the middle ear cavity [31,32], was performed to examine the survival of cell types other than ciliated cells within the transplanted hiPSC-derived AECs (Fig. 6). hiPSC-derived AECs have been reported to express the above markers [16,20,33,34]. KRT5-and HNA-double-positive cells were observed in the post-transplant tissue of all animals with HNA- and Ac-TUB-double-positive cells (n = 3) in the 1- and 2-week groups (Fig. 6a). MUC5AC- and HNA-double-positive cells were found on the middle ear cavity surface in two of three animals in the 1-week group and in one of three animals in the 2-week group (Fig. 6b). KRT5-and MUC5AC-positive cells were found in the normal middle ear mucosa of X-SCID rats (Fig. 6c and d).

4. Discussion

Target cells differentiated from hiPSCs prior to transplantation have shown efficacy for the regeneration of different types of organs, including the cornea [35] and myocardium [36], has recently been proven. Hence, therapy using hiPSCs is expected to provide a new cell source for cell transplantation in patients who experience difficulties in cellular regeneration or autologous transplantation from similar other organs. In this study, we transplanted hiPSC-derived AECs into the middle ear of rats to investigate the conditions necessary for AEC survival.

Previous middle ear mucosa transplantation experiments have primarily focused on autologous transplantation in rabbit models [9,10]. Compared with smaller laboratory animals, rabbits have larger ear bullae, which make surgical procedures, including mucosal dissection, and transplantation [10] easier. In our previous study, we reported on the potential of using middle ear pressure as a measure of gas exchange capacity through the middle ear mucosa [9]. However, we could not use rabbits in this study. The current study requires immunosuppression because transplantation of human-derived cells into an animal model is a xenograft. Because immunosuppression with a drug is insufficient in normal animals in a case of a xenograft, immunodeficient animals were more suitable for the current study. Of the several available immunodeficient animal models, we used X-SCID rats, which have defective immune systems, particularly regarding T, B, and natural killer cell functions [37]. The ear bullae of rats are of a sufficient size to accommodate cell transplantation; additionally, the usefulness of X-SCID rats as models for xenograft experiments for other organs has been reported previously [38,39].

We preliminarily used nude rats as immunodeficient rats (data not shown). However, nude rats were not appropriate for xenograft experiments in the middle ear. No HNA-positive ciliated cells were found on the middle ear cavity surface of the transplanted side in these rats (data not shown). Additionally, only cyst-like engraftments were found in the submucosal tissue of three of the six heads one week after transplantation (data not shown). These results indicate the existence of severe tissue rejection. Nude rats lack the immune response that comes from T-cells [40,41], although the B and NK cells retain normal functions. Therefore, B-cell and NK-cell-mediated immune responses may contribute to the observed

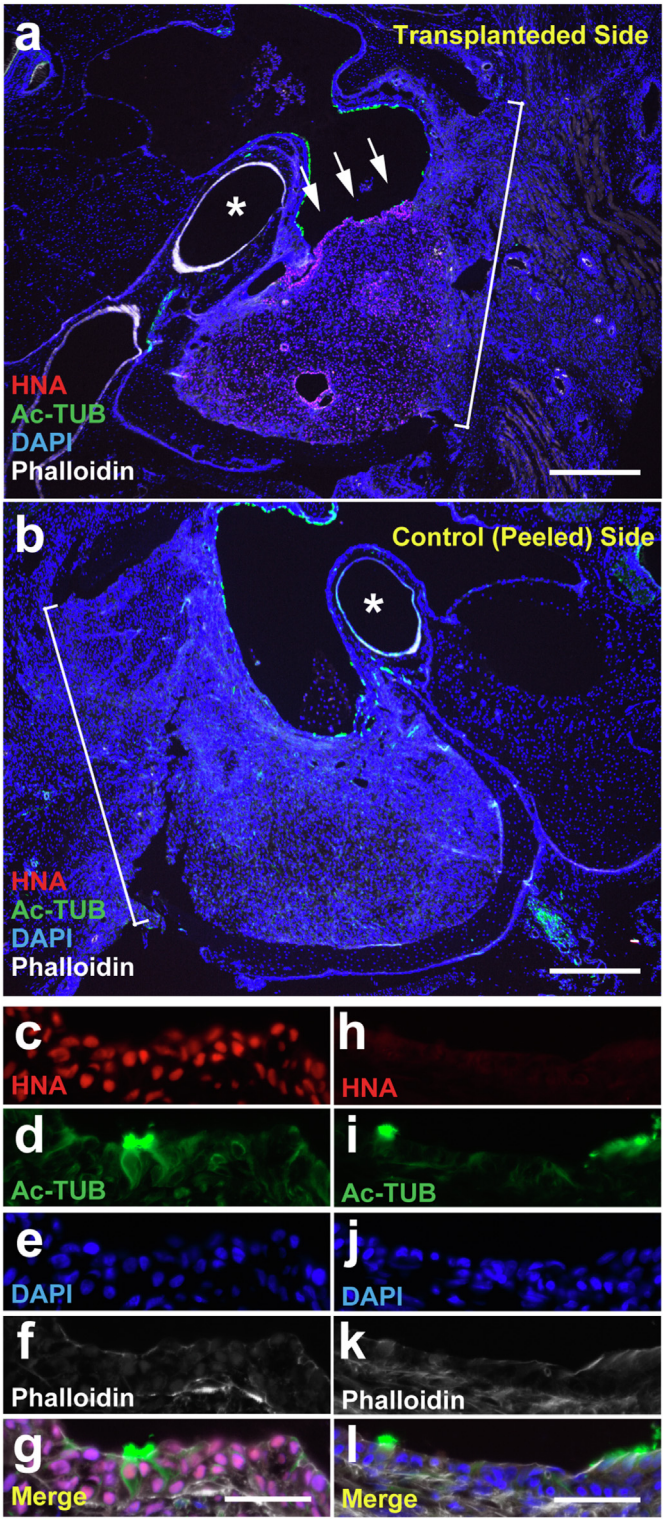

Fig. 4. The engraftment of transplanted cells was observed in the middle ear mucosa of the X-SCID rat 1 week after transplantation. Representative immunofluorescent staining images of the transplanted (a and c–g) and control sides (b and h–l) of the middle ears of the 1-week group. Macroscopic HNA, Ac-TUB, DAPI, and phalloidin staining images (a and b) and microscopic HNA staining (c and h), Ac-TUB staining (d and i), DAPI staining (e and j), phalloidin staining (f and k), and merged (g and l) images are presented. Images c–g and h–l are from same sections, respectively. Ac-TUB- and HNA- double positive cells (arrows in a and c–g, n = 3 out of 6) were observed on the transplanted side. HNA-positive cells were not present on the control side (b and h–l). Scale bar = 500 μm (a and b) and 50 μm (c–g and h–l). Ac-TUB, acetylated α-tubulin; DAPI, 4′,6-diamidino-2-phenylindole; HNA, human nuclear antigen; X-SCID, X-linked severe combined immunodeficient. Asterisks in a and b, stapedial artery; brackets in a and b, surgical window.

immune related rejection within the middle ear cavity. These observations may aid in the selection of immunosuppression methods when allograft transplantation using hiPSCs is clinically performed in the middle ear cavity.

Similar to previous studies using rabbit models [9,10], bone-like tissue growth was observed on the control side of the X-SCID rat middle ear cavity after mucosal defects. On the transplantation side, expansion of the submucosal fibrous layer was observed, which is different from bone thickening observed in the control side (Supplementary Fig. 2). Considering the hardness, the fibrous tissue expansion of the submucosa on the transplantation side was better histological condition than the bony tissue on the control side. However, this was different from previous studies that used autologous cell sheets from the nasal epithelia [9,10]; the studies showed regeneration of almost normal submucosal tissues. This difference may be attributed to the immune response observed in xenograft experiments. However, this may not be a significant problem when the method is clinically applied. In previous studies [9,10], researchers were non-conclusive regarding whether the regenerated tissue originated from the transplanted tissue, or if it was induced from the middle ear mucosa of the recipient. In this study, we confirmed through the detection of HNA that regenerated AECs were derived from transplanted hiPSC-derived AECs.

The number of surviving transplanted cells on the middle ear cavity surface was lower in the 2-week group compared with that in the 1-week group; this decrease may be attributed to the immune response of X-SCID rats to xenograft tissue. Although we found mononuclear cell infiltration on the transplant site at a similar frequency at 1 and 2 weeks, fibrosis at the transplant site seemed more severe at two weeks. This observation suggests that immune response continuously happened at this site. In contrast, the transplantation of similarly prepared hiPSC-derived AECs into the trachea of nude rats with an artificial scaffold [21] caused an increased cell number 2 weeks post-transplantation. This difference indicates increased severity in the immune environment of the middle ear cavity compared with that of the trachea. Another possible reason for the different responses after transplantation is the differing environments of the transplanted sites. In this study, the induction of hiPSC-derived AECs was based on a protocol for inducing lower respiratory epithelial cells, and these cells were not completely similar to the epithelial cells within the middle ear. Therefore, the transplanted cells may not be an appropriate fit for the middle ear environment, and this could have resulted in their decreased numbers. To achieve more efficient regeneration of the middle ear mucosa, it will be necessary to elucidate the specific cellular characteristics of the middle ear mucociliary epithelia and then to correspondingly modify the induction protocol of AECs.

The proportion of ciliated and goblet cells (secretory cells) in the mucociliary epithelia affects its function; additionally, these proportions vary across tissues that include the middle ear, nose, and trachea. Decreased numbers of ciliated cells and increased numbers of goblet cells are associated with many chronic respiratory diseases such as cystic fibrosis, asthma, and chronic otitis media [42–45]. Moreover, the excessive mucus production associated with goblet cell hyperplasia results in repeated tissue damage, repair defects, and mucociliary clearance changes [44]. Therefore, appropriate numbers of goblet cells that secrete inflammatory mediators is necessary to prevent the progression of tissue remodeling [43,46]. Thus, increasing the precision of AEC induction from hiPSCs is necessary to achieve the appropriate proportion of components in the target tissue. Transcriptome and proteome analysis of these tissues may help to elucidate the mechanisms underlying the differences between middle ear, nasal, and tracheal AECs.

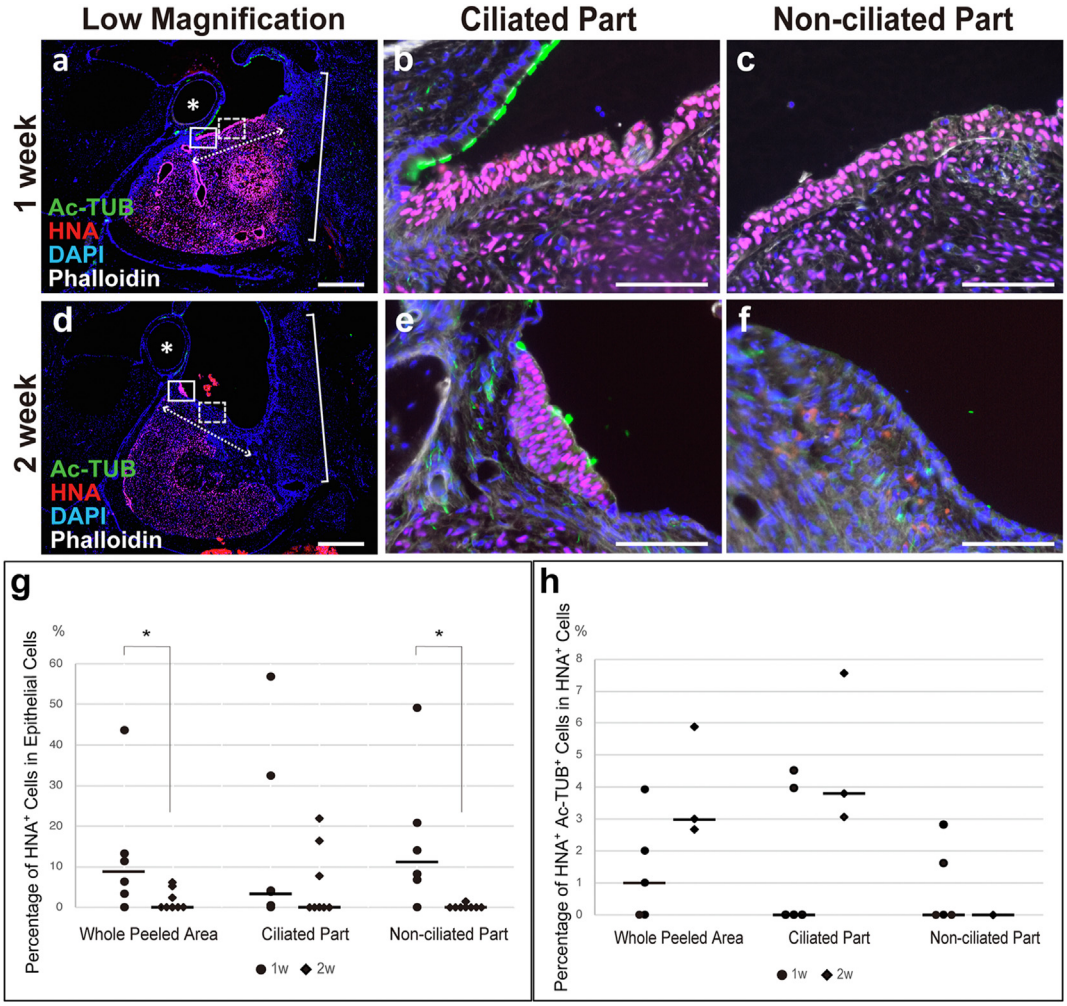

Fig. 5. Transplanted cells mainly survived in the expected ciliated part. Histological sections were stained with anti-acetylated α-tubulin (Ac-TUB) antibody, anti-human nuclear antigen (HNA) antibody, DAPI (4′,6-diamidino-2-phenylindole), and phalloidin (a–f) one (a–c) and two (d–f) weeks after transplantation. b, e (ciliated part) and c, f (non-ciliated part) are magnified images of the solid and dashed boxes in a and d, respectively. The proportion of transplanted cells among epithelial cells within the peeled area (g) and ciliated cells among the transplanted cells (h) was quantified by counting the number of stained cells. The percentage of HNA-positive cells relative to the number of DAPI stained nuclei in the epithelial layer of the whole peeled area and expected non-ciliated part significantly decreased in the 2-week group (g). The percentage of Ac-TUB and HNA double-positive cells in the HNA-positive cells showed an increasing trend in the whole peeled area and expected ciliated part (h). HNA-positive cells hardly survived and no Ac-TUB- and HNA-double-positive cells were observed in the non-ciliated part of the 2-week group (g and h). Scale bars = 500 μm (a and d) and 100 μm (b, c, e, and f). Asterisks in a and d, stapedial artery; brackets in a and d, surgical window; dotted double arrows in a and d, apical surface of the peeled area. Dashes in graphs, median (g, h).

Ciliated cells are essential for mucociliary clearance [47] and are differentiated from basal cells [48]. In this study, we confirmed basal cells in the transplanted cells and the proportion of ciliated cells in the transplanted cells tended to increase in two weeks after transplantation compared with those in one week, although the net number of transplanted cells decreased. These observations seemed to be limited to areas abundant in ciliated cells prior to the mucosal damage (Fig. 5). Moreover, the decrease in the number of whole transplanted cells mainly occurred in the expected non-ciliated part (Fig. 5g), and the total number of transplanted cells seemed to be maintained within the expected ciliated part. These results suggest that the transplantation site is important for achieving efficient regeneration of ciliated cells, and that the environment of the recipient site may affect the survival of transplanted hiPSC-derived ciliated cells (Fig. 7). Generally, the microenvironment has essential roles in stabilizing transplanted cells. For example, transplanted hematopoietic stem cells require the environment of bone marrow to be functional. They can reconstitute the hematopoietic compartments of a host only after homing into host bone marrow [49]. Similarly, successful transplantation of induced AECs into a middle ear may require an appropriate environment. It is crucial to select a proper location for epithelial-cell transplantation because they are hard to migrate, unlike hematopoietic cells.

This study is the first trial of hiPSC-derived AECs transplantation onto the surface of the middle ear cavity. Transplantation of cells sometimes raises safety issues. However, from the viewpoints of the environment, the middle ear cavity is originally an environment in which tumor formation is unlikely to occur, which is supported by clinical facts that primary cancer of the middle ear is rare [50]. Regarding the characteristics of transplanted cells, transplanted cells have a very low probability of producing tumors because hiPSC-derived AECs are differentiated cells, and immature cells have been removed by magnetically activated cell sorting purification during the induction process. If transplanted hiPSC-derived AECs become more stable in the future following protocol modification, this experimental model may be used as a humanized middle ear mucosa model. This model may also be useful for elucidating the pathogenesis of intractable otitis media and for the developing drugs to manage the condition.

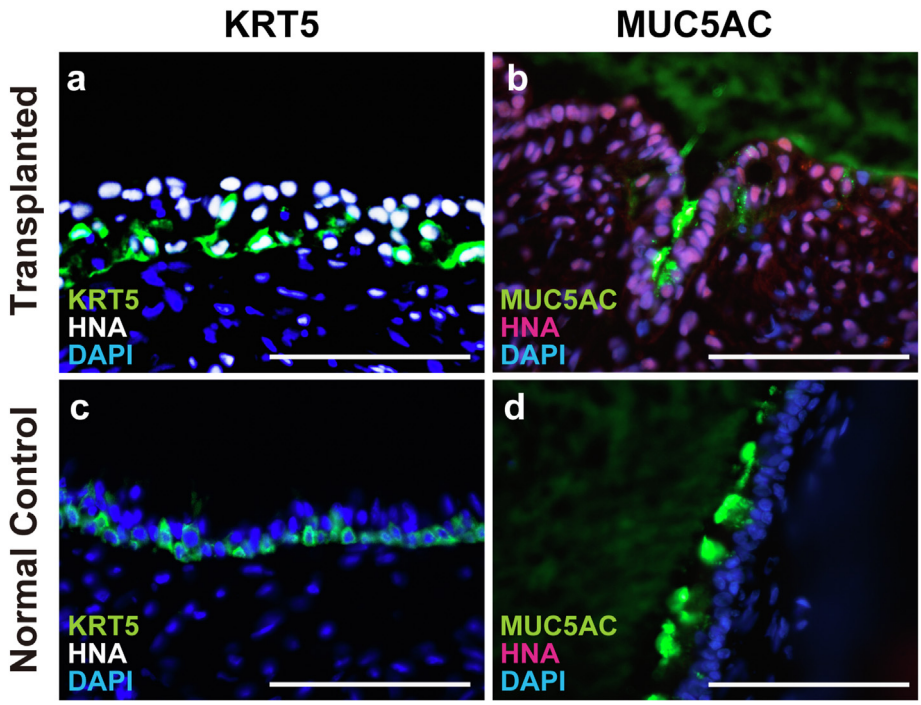

Fig. 6. Airway epithelial component cells other than ciliated cells were observed in transplanted cells. The sections of transplanted (a and b) and control (c and d) middle ears of X-SCID rats were immunostained with anti-human nuclear antigen (HNA) and DAPI. Double immunostaining was performed using anti-cytokeratin5 (KRT5, a basal cell marker, a and c), or anti-mucin 5AC (MUC5AC, a goblet cell marker, b and d) antibodies. KRT5 and MUC5AC positive cells were observed in the transplanted and normal middle ear mucosa of X-SCID rats. Scale bars = 100 μm. HNA, human nuclear antigen; KRT5, cytokeratin 5; MUC5AC, mucin 5AC; X-SCID, X-linked severe combined immunodeficient.

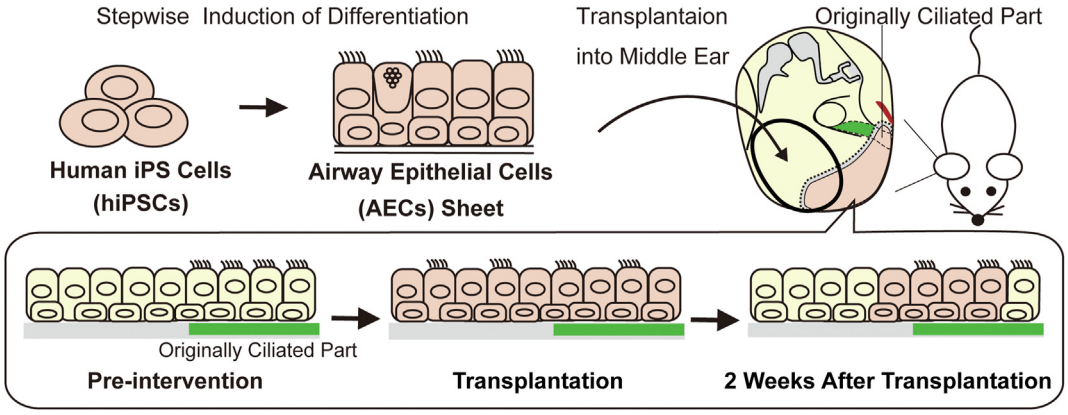

Fig. 7. Summary diagram of transplantation experiment. To evaluate a new cell source for mucosal regeneration after middle ear surgery, AECs derived from hiPSCs were transplanted into the middle ear of immunodeficient rats. The cells transplanted into the defect of the mucosa survived mainly in the originally ciliated part, suggesting a microenvironmental influence on the success of transplantation. AECs, airway epithelial cells; hiPSCs, human induced pluripotent stem cells.

This study has some limitations. First, assessing long-term cell dynamics and functional analysis was difficult because of the immune response caused by xenotransplantation. Therefore, stronger immunosuppression may be necessary to analyze the microenvironment required for ciliated cell differentiation and maintenance. Second, avoiding the proliferation of HNA-positive mesenchymal cells, which are derived from transplanted cells, in the submucosa needs to be examined in the future. Third, the size of the rats' middle ear prevents functional analysis of transplanted cells. One possible solution is to develop an in vivo model using the recently developed X-SCID rabbit to measure middle ear pressure and evaluate functions such as cilia movement in the transplanted tissue [51].

5. Conclusions

We developed a fundamental method for the transplantation of hiPSC-derived AECs into the middle ear mucosa. Furthermore, we confirmed hiPSC-derived AEC survival on the surface of the middle ear cavity of X-SCID rats. Increasing the survival rate of transplanted cells needs to be examined in the future in order to adequately evaluate the function of the middle ear after cell transplantation therapy.

Declaration of competing interest

The authors declare no conflicts of interest.

Acknowledgments

We thank Ms. Keiko Okamoto-Furuta and Mr. Haruyasu Kohda from the Division of Electron Microscopic Study, Center for Anatomical Studies, Graduate School of Medicine, Kyoto University for their technical support with electron microscopy. We also thank Professor Tomoji Mashimo at the National BioResource Project - Rat (http://www.anim.med.kyoto-u.ac.jp/NBR/) for providing the rat strain (F344-*Il2rg*^{em1lexas}, NBRP No. 0883). We would like to thank Editage (www.editage.com) and Georgia Lenihan-Geels, PhD, from Edanz (https://jp.edanz.com/ac) for editing a draft of this manuscript.

This research was supported by The Jikei University Research Fund for Graduate Students and the Alumni Otolaryngology Fund from the Department of Otolaryngology Head and Neck Surgery, Graduate School of Medicine, Kyoto University.

Appendix A. Supplementary data

Supplementary data to this article can be found online at https://doi.org/10.1016/j.reth.2022.01.001.

References

[1] Padurariu S, Röösli C, Røge R, Stensballe A, Vyberg M, Huber A, et al. On the functional compartmentalization of the normal middle ear. Morpho-histological modelling parameters of its mucosa. Hear Res 2019;378:176–84. https://doi.org/10.1016/j.heares.2019.01.023.
[2] Ars B, Dirckx J, Ars-Piret N, Buytaert J. Insights in the physiology of the human mastoid: message to the surgeon. J Int Adv Otol 2012;8:296–310.
[3] Hentzer E. Ultrastructure of the middle ear mucosa. Acta Otolaryngol Suppl 1984;414:19–27.
[4] Marchioni D, Alicandri-Ciufelli M, Molteni G, Artioli FL, Genovese E, Presutti L. Selective epitympanic dysventilation syndrome. Laryngoscope 2010;120:1028–33. https://doi.org/10.1002/lary.20841.
[5] Song CI, Hong HR, Yoon TH. Influence of middle ear mucosal condition on post-tympanoplasty audiologic outcome. Eur Arch Oto-Rhino-Laryngol 2016;273:581–5. https://doi.org/10.1007/s00405-015-3590-0.
[6] Jang CH, Ahn SH, Kim GH. Antifibrotic effect of dexamethasone/alginate-coated silicone sheet in the abraded middle ear mucosa. Int J Biol Macromol 2016;93:1612–9. https://doi.org/10.1016/j.ijbiomac.2016.04.033.
[7] Mouna B, Khalifa M, Ghammem M, Limam M, Meherzi A, Kermani W, et al. Cartilage and fascia graft in type 1 tympanoplasty: comparison of anatomical and audiological results. J Craniofac Surg 2019;30:e297–300. https://doi.org/10.1097/scs.0000000000005278.
[8] Yamamoto K, Yamato M, Morino T, Sugiyama H, Takagi R, Yaguchi Y, et al. Middle ear mucosal regeneration by tissue-engineered cell sheet transplantation. NPJ Regen Med 2017;2:6. https://doi.org/10.1038/s41536-017-0010-7.
[9] Yamamoto K, Hama T, Yamato M, Uchimizu H, Sugiyama H, Takagi R, et al. The effect of transplantation of nasal mucosal epithelial cell sheets after middle ear surgery in a rabbit model. Biomaterials 2015;42:87–93. https://doi.org/10.1016/j.biomaterials.2014.11.037.
[10] Yaguchi Y, Murakami D, Yamato M, Hama T, Yamamoto K, Kojima H, et al. Middle ear mucosal regeneration with three-dimensionally tissue-engineered autologous middle ear cell sheets in rabbit model. J Tissue Eng Regen Med 2016;10:E188–94. https://doi.org/10.1002/term.1790.
[11] Hama T, Yamamoto K, Yaguchi Y, Murakami D, Sasaki H, Yamato M, et al. Autologous human nasal epithelial cell sheet using temperature-responsive culture insert for transplantation after middle ear surgery. J Tissue Eng Regen Med 2017;11:1089–96. https://doi.org/10.1002/term.2012.
[12] Nakatsuji N, Nakajima F, Tokunaga K. HLA-haplotype banking and iPS cells. Nat Biotechnol 2008;26:739–40. https://doi.org/10.1038/nbt0708-739.
[13] Okita K, Matsumura Y, Sato Y, Okada A, Morizane A, Okamoto S, et al. A more efficient method to generate integration-free human iPS cells. Nat Methods 2011;8:409–12. https://doi.org/10.1038/nmeth.1591.
[14] Taylor CJ, Peacock S, Chaudhry AN, Bradley JA, Bolton EM. Generating an iPSC bank for HLA-matched tissue transplantation based on known donor and recipient HLA types. Cell Stem Cell 2012;11:147–52. https://doi.org/10.1016/j.stem.2012.07.014.
[15] Ryan AF, Nasamran CA, Pak K, Draf C, Fisch KM, Webster N, et al. Single-cell transcriptomes reveal a complex cellular landscape in the middle ear and differential capacities for acute response to infection. Front Genet 2020;11:358. https://doi.org/10.3389/fgene.2020.00358.
[16] Zaragosi LE, Deprez M, Barbry P. Using single-cell RNA sequencing to unravel cell lineage relationships in the respiratory tract. Biochem Soc Trans 2020;48:327–36. https://doi.org/10.1042/bst20191010.
[17] Ruiz García S, Deprez M, Lebrigand K, Cavard A, Paquet A, Arguel MJ, et al. Novel dynamics of human mucociliary differentiation revealed by single-cell RNA sequencing of nasal epithelial cultures. Development 2019;146:177428. https://doi.org/10.1242/dev.177428.
[18] Lim DJ, Hussl B. Human middle ear epithelium. An ultrastructural and cytochemical study. Arch Otolaryngol 1969;89:835–49. https://doi.org/10.1001/archotol.1969.00770020837009.
[19] Gotoh S, Ito I, Nagasaki T, Yamamoto Y, Konishi S, Korogi Y, et al. Generation of alveolar epithelial spheroids via isolated progenitor cells from human pluripotent stem cells. Stem Cell Reports 2014;3:394–403. https://doi.org/10.1016/j.stemcr.2014.07.005.
[20] Konishi S, Gotoh S, Tateishi K, Yamamoto Y, Korogi Y, Nagasaki T, et al. Directed induction of functional multi-ciliated cells in proximal airway epithelial spheroids from human pluripotent stem cells. Stem Cell Reports 2016;6:18–25. https://doi.org/10.1016/j.stemcr.2015.11.010.
[21] Okuyama H, Ohnishi H, Nakamura R, Yamashita M, Kishimoto Y, Tateya I, et al. Transplantation of multiciliated airway cells derived from human iPS cells using an artificial tracheal patch into rat trachea. J Tissue Eng Regen Med 2019;13:1019–30. https://doi.org/10.1002/term.2849.
[22] Li P, Ding D, Gao K, Salvi R. Standardized surgical approaches to ear surgery in rats. J Otolaryngol 2015;10:72–7. https://doi.org/10.1016/j.joto.2015.03.004.
[23] Mülazımoğlu S, Ocak E, Kaygusuz G, Gökcan MK. Retroauricular approach for targeted cochlear therapy experiments in wistar albino rats. Balkan Med J 2017;34:200–5. https://doi.org/10.4274/balkanmedj.2016.0226.
[24] Judkins RF, Li H. Surgical anatomy of the rat middle ear. Otolaryngol Head Neck Surg 1997;117:438–47. https://doi.org/10.1016/s0194-5998(97)70011-1.
[25] Gibbons IR, Rowe AJ. Dynein: a protein with adenosine triphosphatase activity from cilia. Science 1965;149:424–6. https://doi.org/10.1126/science.149.3682.424.
[26] Maeda S, Mogi G, Oh M. Fine structures of the normal mucosa in developing rat middle ear. Ann Otol Rhinol Laryngol 1976;85:1–19. https://doi.org/10.1177/00034894760855s201.
[27] Gras D, Chanez P, Vachier I, Petit A, Bourdin A. Bronchial epithelium as a target for innovative treatments in asthma. Pharmacol Ther 2013;140:290–305. https://doi.org/10.1016/j.pharmthera.2013.07.008.
[28] Kotton DN, Morrisey EE. Lung regeneration: mechanisms, applications and emerging stem cell populations. Nat Med 2014;20:822–32. https://doi.org/10.1038/nm.3642.
[29] Luo W, Yi H, Taylor J, Li JD, Chi F, Todd NW, et al. Cilia distribution and polarity in the epithelial lining of the mouse middle ear cavity. Sci Rep 2017;7:45870. https://doi.org/10.1038/srep45870.
[30] Tucker AS, Dyer CJ, Fons Romero JM, Teshima THN, Fuchs JC, Thompson H. Mapping the distribution of stem/progenitor cells across the mouse middle ear during homeostasis and inflammation. Development 2018;145:154393. https://doi.org/10.1242/dev.154393.
[31] Kerschner JE, Tripathi S, Khampang P, Papsin BC. MUC5AC expression in human middle ear epithelium of patients with otitis media. Arch Otolaryngol Head Neck Surg 2010;136:819–24. https://doi.org/10.1001/archoto.2010.123.
[32] Chen YP, Tong HH, James MA, Demaria TF. Detection of mucin gene expression in normal rat middle ear mucosa by reverse transcriptase-polymerase chain reaction. Acta Otolaryngol 2001;121:45–51. https://doi.org/10.1080/000164801300006263.
[33] Rock JR, Onaitis MW, Rawlins EL, Lu Y, Clark CP, Xue Y, et al. Basal cells as stem cells of the mouse trachea and human airway epithelium. Proc Natl Acad Sci U S A 2009;106:12771–5. https://doi.org/10.1073/pnas.0906850106.
[34] Lin J, Tsuprun V, Kawano H, Paparella MM, Zhang Z, Anway R, et al. Characterization of mucins in human middle ear and Eustachian tube. Am J Physiol Lung Cell Mol Physiol 2001;280:L1157–67. https://doi.org/10.1152/ajplung.2001.280.6.L1157.
[35] Hayashi R, Ishikawa Y, Sasamoto Y, Katori R, Nomura N, Ichikawa T, et al. Co-ordinated ocular development from human iPS cells and recovery of corneal function. Nature 2016;531:376–80. https://doi.org/10.1038/nature17000.
[36] Masumoto H, Ikuno T, Takeda M, Fukushima H, Marui A, Katayama S, et al. Human iPS cell-engineered cardiac tissue sheets with cardiomyocytes and vascular cells for cardiac regeneration. Sci Rep 2014;4:6716. https://doi.org/10.1038/srep06716.
[37] Mashimo T, Takizawa A, Voigt B, Yoshimi K, Hiai H, Kuramoto T, et al. Generation of knockout rats with X-linked severe combined immunodeficiency (X-SCID) using zinc-finger nucleases. PLoS One 2010;5:e8870. https://doi.org/10.1371/journal.pone.0008870.
[38] Nishimura K, Doi D, Samata B, Murayama S, Tahara T, Onoe H, et al. Estradiol facilitates functional integration of iPSC-derived dopaminergic neurons into striatal neuronal circuits via activation of integrin α5β1. Stem Cell Reports 2016;6:511–24. https://doi.org/10.1016/j.stemcr.2016.02.008.
[39] Samata B, Kikuchi T, Miyawaki Y, Morizane A, Mashimo T, Nakagawa M, et al. X-linked severe combined immunodeficiency (X-SCID) rats for xeno-transplantation and behavioral evaluation. J Neurosci Methods 2015;243:68–77. https://doi.org/10.1016/j.jneumeth.2015.01.027.
[40] Vos JG, Kreeftenberg JG, Kruijt BC, Kruizinga W, Steerenberg P. The athymic nude rat. II. Immunological characteristics. Clin Immunol Immunopathol 1980;15:229–37. https://doi.org/10.1016/0090-1229(80)90033-1.

[41] Hougen HP. The athymic nude rat. Immunobiological characteristics with special reference to establishment of non-antigen-specific T-cell reactivity and induction of antigen-specific immunity. APMIS Suppl 1991;21:1–39.
[42] Cohn L. Mucus in chronic airway diseases: sorting out the sticky details. J Clin Invest 2006;116:306–8. https://doi.org/10.1172/jci27690.
[43] Curran DR, Cohn L. Advances in mucous cell metaplasia: a plug for mucus as a therapeutic focus in chronic airway disease. Am J Respir Cell Mol Biol 2010;42:268–75. https://doi.org/10.1165/rcmb.2009-0151TR.
[44] Merigo F, Benati D, Piacentini G, Boner A, Sbarbati A. The ultrastructure of nasal mucosa in children with asthma. Ultrastruct Pathol 2002;26:293–8. https://doi.org/10.1080/01913120290104566.
[45] Tos M, Bak-Pedersen K. Density of goblet cells in chronic secretory otitis media: findings in a biopsy material. Laryngoscope 1975;85:377–83. https://doi.org/10.1288/00005537-197502000-00015.
[46] Whitsett JA. Airway epithelial differentiation and mucociliary clearance. Ann Am Thorac Soc 2018;15:S143–8. https://doi.org/10.1513/AnnalsATS.201802-128AW.
[47] Zhou F, Narasimhan V, Shboul M, Chong YL, Reversade B, Roy S. Gmnc is a master regulator of the multiciliated cell differentiation program. Curr Biol 2015;25:3267–73. https://doi.org/10.1016/j.cub.2015.10.062.
[48] Tadokoro T, Wang Y, Barak LS, Bai Y, Randell SH, Hogan BL. IL-6/STAT3 promotes regeneration of airway ciliated cells from basal stem cells. Proc Natl Acad Sci U S A 2014;111:E3641–9. https://doi.org/10.1073/pnas.1409781111.
[49] Podestà M. Transplantation hematopoiesis. Curr Opin Hematol 2001;8:331–6. https://doi.org/10.1097/00062752-200111000-00003.
[50] Qiu K, Pang W, Qiu J, Li J, Cheng D, Rao Y, et al. Evaluating the prognostic contributions of TNM classifications and building novel staging schemes for middle ear squamous cell carcinoma. Cancer Med 2021;10:7958–67. https://doi.org/10.1002/cam4.4306.
[51] Hashikawa Y, Hayashi R, Tajima M, Okubo T, Azuma S, Kuwamura M, et al. Generation of knockout rabbits with X-linked severe combined immunodeficiency (X-SCID) using CRISPR/Cas9. Sci Rep 2020;10:9957. https://doi.org/10.1038/s41598-020-66780-6.